UHMET 89-01

EQUATORIAL DISTURBANCES AND MONSOONS DURING THE 82-83 ENSO

by Takio Murakami

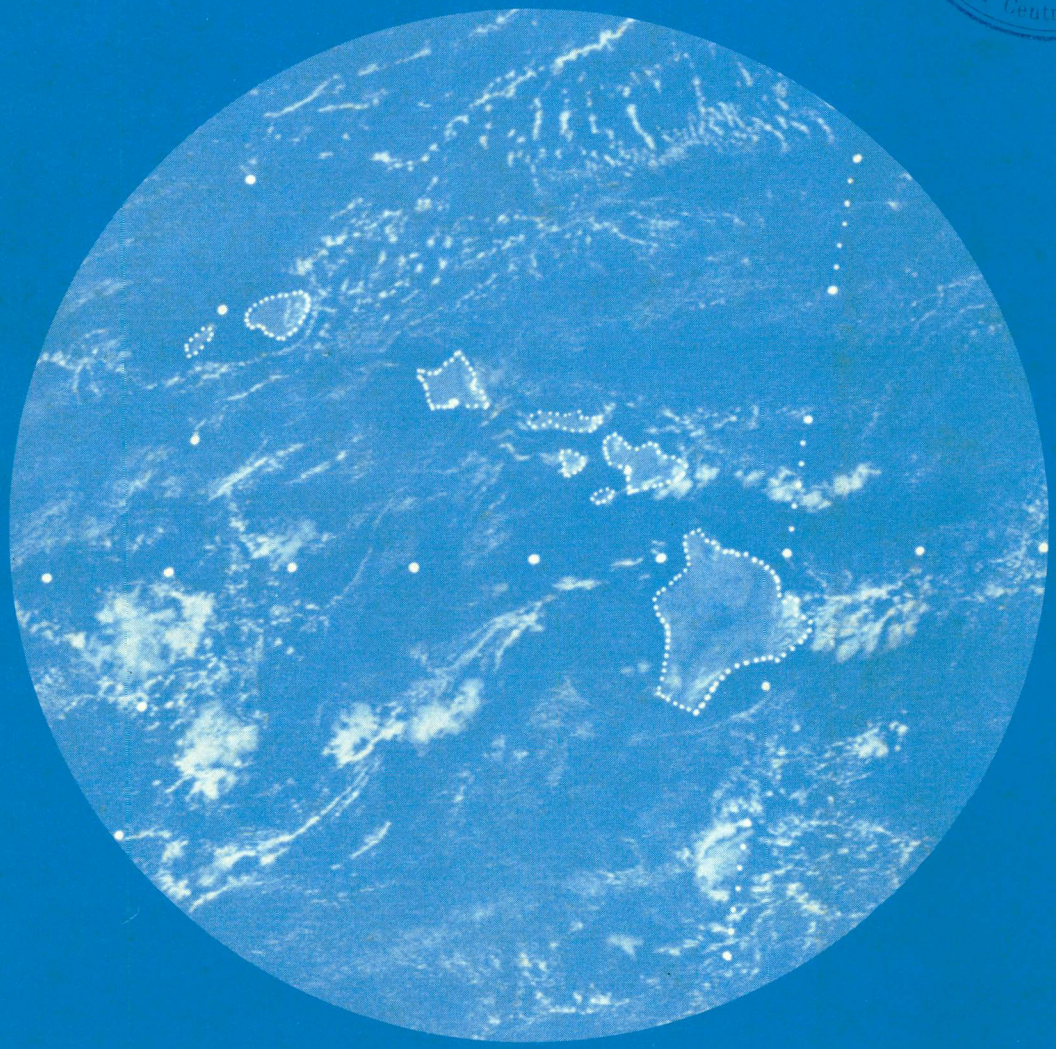

Supported by
National Science Foundation, Washington, D.C.
under Grant No. ATM-8609968

April 1989

Department of Meteorology, University of Hawaii

DEPARTMENT OF METEOROLOGY, UNIVERSITY OF HAWAII
CONTRIBUTIONS AND TECHNICAL REPORTS
LIST NO. 8
1 January 1987 to 31 December 1988

CONTRIBUTIONS

85-05 Murakami, T., and [K. Ninomiya], 1987: Baiu over Japan. In Monsoon Meteorology. C.-P. Chang and T. Krishnamurti, eds., New York, Oxford Univ. Press, pp. 93-122.

85-08 Murakami, T., 1987: Orography and the monsoons. Chapter 12, Monsoons, J. Fein and P. Stephens, Eds., New York, Wiley, pp. 331-364.

85-09 Chu, P.-S., and R. W. Katz, 1987: Measures of predictability with application to the Southern Oscillation. Mon. Wea. Rev., 115, 1542-1549.

85-10 Chen, Y.-L., 1987: Thermodynamic effects of mesoscale convective systems on the environment over the eastern Atlantic. J. Meteor. Soc. Japan, 65, 391-400.

86-02 Murakami, T., 1986: 30-60 day atmospheric teleconnection patterns during the Southern Hemisphere summer. Second International Conference on Southern Hemisphere Meteorology, Wellington, New Zealand, December 1-5, AMS, Boston, MA, 336-338.

86-05 Murakami, T., 1986: 30-60 day atmospheric teleconnection patterns during the Northern Hemisphere summer. International Conference on Monsoon and Mesoscale Meteorology, Taipei, Taiwan, November 4-7, 1986, AMS, Boston, MA, 258-262.

86-07 Daniels, A., 1987: Diffusion and emission of smoke from agricultural burning in Hawaii. Water, Air and Soil Pollution, 34, 111-124.

86-08 Murakami, T., 1987: Intraseasonal atmospheric teleconnection patterns during Northern Hemispheric summer. Mon. Wea. Rev., 113, 2133-2154.

86-09 Takahashi, T., 1986: Wind shear effect on water accumulation and rain duration in Hawaiian clouds. J. Meteor. Soc. Japan, 64, 575-584.

87-01 Sumathipala, W. L., and T. Murakami, 1986: Large-scale aspects of active and break monsoons over southeast Asia during the 1979 summer. Papers in Meteorological Research, (Taiwan), 9, 105-116.

87-02 Sumathipala, W. L., 1987: Eastern North Pacific hurricanes of 1979 and the Asian summer monsoon. 17th Conference on Hurricanes and Tropical Meteorology, Miami, FL, April 7-10, AMS, Boston, MA, 142-144.

Contributions (continued)

87-03 Shrestha, M. L., and T. Murakami, 1987: Intraseasonal fluctuations in low-level meridional winds over the Indian Ocean and monsoonal convection over South Asia. Tellus, 40-A, 120-132.

87-04 Lander, M. A., 1987: An investigation of the large-scale changes of the wind, sea level pressure and clouds associated with tropical cyclone twins symmetrical about the equator in the western Pacific. Preprints, 17th Conference on Hurricanes and Tropical Meteorology, Miami, FL, April 7-10, 1987, AMS, 212-214.

87-05 Chen, Y.-L., 1987: Life cycle effects of cloud clusters on the vertical distributions of convective heating and drying during Phase III of GATE. Preprints, 17th Conference on Hurricanes and Tropical Meteorology, Miami, FL, April 7-10, AMS, 15-18.

87-07 Wang, X., and T. Murakami, 1987: Intraseasonal meridional surges and equatorial convections during the Southern Hemisphere summer. J. Meteor. Soc. Japan, 65, No. 5.

87-08 Lander, M. A., and M. L. Morrissey, 1987: Unexpected duplicate ship reports in the Comprehensive Ocean-Atmosphere Data Set (COADS). Tropical Ocean Atmosphere Newsletter, 38, 5-7.

87-09 Murakami, T., 1988: Intraseasonal atmospheric teleconnection patterns during the Northern Hemisphere winter. J. Climate, 1, 117-131.

87-10 Sumathipala, W. L., and T. Murakami, 1987: Intraseasonal fluctuations in low-level meridional winds over the South China Sea and the western Pacific and monsoonal convection over Indonesia and northern Australia. Tellus, 40A, 205-219.

87-13 Wang, B., 1988: The dynamics of tropical low frequency waves: An analysis of moist Kelvin waves. J. Atmos. Sci., 45, 2051-2065.

87-15 Chen, Y.-L., 1988: Life cycle effects of cloud clusters on the moisture distribution over the eastern Atlantic, J. Meteor. Soc. Japan, 66, No. 2.

87-16 Morrissey, M. L., and M. A. Lander, 1988: A preliminary evaluation of ship data in the equatorial western Pacific. J. Atmos. Ocean Tech., 5, 251-258.

88-01 Wang, X., and T. Murakami, 1988: Intraseasonal disturbance activity before, during, and after the 1982/1983 ENSO, J. Atmos. Sci., 45, No. 24, 3754-3770.

Contributions (continued)

88-03 Wang, B., 1988: Comments on "An air-sea interaction model of intraseasonal oscillations in the tropics." J. Atmos. Sci., 45, 3521-3525.

88-19 Takahashi, T., 1988: Long lasting trade wind rain showers in a three-dimensional model, J. Atmos. Sci., 45, 3333-3353.

TECHNICAL REPORTS

UHMET 87-01 Sadler, J. C., M. A. Lander, A. M. Hori, and L. K. Oda, 1987: Tropical marine climatic atlas. Volume I. Indian Ocean and Atlantic Ocean. NOAA Cooperative Agreement NA85ABH00032.

UHMET 87-02 Sadler, J. C., M. A. Lander, A. Hori, and L. K. Oda, 1987: Tropical marine climatic atlas. Volume II. Pacific Ocean. NOAA Cooperative Agreement NA85ABH00032.

UHMET 88-01 Menon, P., 1988: Indoor spatial monitoring of combustion generated pollutants (TSP, CO, and BaP) by Indian cookstoves. 199 pp.

UHMET 88-02 Murakami, T., and W. L. Sumathipala, 1988: Equatorward surges, equatorial westerlies and convection on interannual and intraseasonal time scales. NSF Grant No. ATM-8609968, 56 pp.

UHMET 88-03 Murakami, T., and W. L. Sumathipala, 1988: Relationship between outgoing longwave radiation and sea surface temperature on interannual time scales. NSF Grant No. ATM-8609968, 27 pp.

OTHER PUBLICATIONS BY DEPARTMENT OF METEOROLOGY STAFF

Lander, M. A., and M. L. Morrissey, 1988: Do equatorial westerlies precede the El Nino?. TOAN.

Murakami, T., 1986: Monsoon (in Japanese). Tokyo, Japan, 201 pp.

Schroeder, T., 1987: "VOG" in Hawaiian Eruptions. Univ. Hawaii Foundation.

Takahashi, T., 1987: Hawaiian hailstones--30 January 1985. Bull. Amer. Meteor. Soc., 68, 1530-1534.

UHMET89-01

Equatorial Disturbances and Monsoons during the 1982-83 ENSO[1]

by
Takio Murakami
Department of Meteorology
University of Hawaii

Supported by
National Science Foundation, Washington, D. C.
under Grant No. ATM-8609968

April 1989

---

[1] Report No. UHMET89-01, Department of Meteorology, University of Hawaii, Honolulu, Hawaii

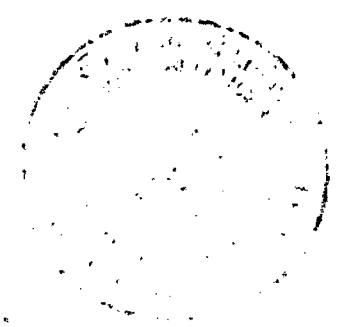

Table of Contents

ABSTRACT

Data used in this study, as well as the symbols and acronyms, are the same as those in UHMET88-02 (Murakami and Sumathipala, 1988a). Interannual modes are described in terms of three-month running mean anomaly winds (u", v"), outgoing longwave radiation (OLR"), and sea surface temperature ($T_*^{"}$). Normal atmospheric monsoon circulations are defined by long-term average winds (u_n, v_n) computed every month from January to December. Daily winds are grouped into three frequency bands, i.e., 30-60 day filtered winds (u_L, v_L); 7-20 day filtered winds (u_M, v_M); and 2-6 day filtered winds (u_S, v_S). Three-month running mean anomaly kinetic energy (signified as $K_L^{"}$, $K_M^{"}$, and $K_S^{"}$, respectively) is then introduced as a measure of interannual variation of equatorial disturbance activity. Interestingly, all of these $K_L^{"}$, $K_M^{"}$, and $K_S^{"}$ perturbations propagate slowly eastward with same phase speed (0.3 m s^{-1}) as ENSO modes. Associated with this eastward propagation is a positive (negative) correlation between interannual disturbance activity ($K_L^{"}$, $K_M^{"}$, $K_S^{"}$) and interannual u" (OLR") modes. Namely, ($K_L^{"}$, $K_M^{"}$, $K_S^{"}$) becomes more pronounced than usual nearly simultaneously with the arrival of westerly u" and negative OLR" (above normal convection). In these disturbed areas with ($K_L^{"}$, $K_M^{"}$, $K_S^{"} > 0$), upper ocean mixing tends to increase, resulting in decreased sea surface temperature, i.e., $T_*^{"} \leq 0$. Thus, groups (not individual) of equatorial disturbances appear to play an important role in determining $T_*^{"}$ variations on interannual time scales. Highest $T_*^{"}$ occurs about 3 months prior to the lowest OLR" (convection) due primarily to radiational effects. This favors the eastward propagation of ENSO modes. The interannual $T_*^{"}$ variations are also controlled by the prevailing monsoonal zonal winds u_n, as well as the zonal advection of sea surface temperature on interannual time scales. Over the

central Pacific, all of the above mentioned physical processes contribute to the intensification of eastward propagating ENSO modes. Over the Indian Ocean, on the other hand, some of the physical processes become insignificant, or even compensated for by other processes. This results in less pronounced ENSO modes over the Indian Ocean.

1. Introduction

Recently, Murakami and Sumathipala (1988a) investigated the relationship between ENSO and equatorial westerly bursts. For brevity, this paper will hereafter be referred to as MSA. (See also Appendix for acronyms and symbols used in this study.) In MSA some of the characteristic features of the ENSO were described in terms of three-month running mean anomalies, which were signified as u", v", OLR", and T_*'', respectively. Daily 850 mb winds and OLR data were subjected to a band-pass filter to obtain climatological information on intraseasonal equatorial disturbances. These filtered data were denoted as u_S, v_S, and OLR_S (2-6 day); u_M, v_M, and OLR_M (7-20 day); and u_L, v_L, OLR_L (30-60 day); respectively. Thus, these intraseasonal perturbations are clearly separate from interannual ENSO modes whose time scales are longer than three months. Of course, (u_L, u_M, u_S) westerly bursts represent only a part of equatorial (u_L, v_L, OLR_L), (u_M, v_M, and OLR_M), and (u_S, v_S, and OLR_S) disturbances. An attempt was then made to determine the difference in space structure of equatorial disturbances with different periodicities. Because of the difference in time and space scales, there exists no direct correlation between individual equatorial disturbances and the interannual ENSO modes. However, this does not rule out the possibility that equatorial disturbances can interact with interannual modes. This possibility will be examined in Section 3.

One of the primary objectives of this study is to investigate the association of ENSO modes with the interannual variations of monsoon activity over the India-Malaysia-Indonesia-Australia region. Meehl (1987) and Yasunari (1988) demonstrated the biennial nature of the eastward propagating interannual signal which involves a modulation of the annual cycle. It includes QBO (Quasi-Biennial Oscillation)-type features that continually evolve throughout the annual cycle from one year to the next as a consequence of the east-west circulation between the Indian and

Pacific sectors, and the associated ocean-atmosphere interaction. Meehl (1987) defined relatively strong and weak monsoon years from an index of Indian monsoon rainfall. This is deemed to be an appropriate starting point to examine the seasonal cycle because the mean convective maximum is stronger in its southeastward traverse from northern summer to northern winter than during the northwestward return excursion in the other half of the year over the Indian-Pacific tropics. As the annual cycle proceeds in a "strong monsoon" year, regions of above normal convection move from India southeastward to the maritime continent and northern Australia, where the Southern Hemisphere summer monsoon becomes more active than usual. The warmer SSTs ahead of the convective maximum contribute to maintaining the strong convection as it moves eastward. The time lag between the highest SST and maximum convection is about 3 months (Murakami and Sumathipala, 1988b; MSB). Over the Australian monsoon region, strong low-level westerlies and associated monsoon disturbances appear to contribute to an increase in upper ocean mixing and greater heat removal from the ocean surface. This results in cooler SSTs over the Australian monsoon region. Strong convection then becomes established over the warmer water in the SPCZ (South Pacific Convergence Zone) region during late northern winter and spring (around April). As relatively greater convection is established in the SPCZ, lower surface pressure is associated with anomalous cyclonic flow. To the east of the SPCZ, anomalous northerly winds contribute to the inducement of warm SST advection from the tropics. Thus, T_*'' tends to become anomalously high to the east of the SPCZ. The low-pressure gradient would also be conducive to equatorial westerly wind anomalies (u") east of New Guinea.[2] At this time, an anomalous east-west vertical overturning develops along the equator

---

[2] These westerly wind anomalies, which are of interannual time scales, are distinctly different from transient westerly bursts, which as claimed by Lukas et al. (1984), excite fast moving oceanic Kelvin waves and initiate El Nino in the eastern equatorial Pacific.

with an updraft leg dominating over the eastern Pacific and a downdraft branch covering the Indian Ocean. Consequently, the Indian monsoon becomes less active than normal. This corresponds to the transition from a relatively strong monsoon year to a relatively weak monsoon year. The relatively weaker convective maximum then moves from India eastward to the Pacific during the course of a "weak" annual cycle with opposite conditions than those prescribed during a "strong" annual cycle. This completes the interannual ENSO cycle.

The set of interactions described above presents a coherent composite picture of the processes involved with the entire ocean-atmosphere coupled system in the Indian and Pacific sectors. This ocean-atmosphere coupled system is nearly identical to that proposed originally by Meehl (1987), although a slight modification has been made by referring to the recent studies by Murakami and Sumathipala [1988a (MSA); 1988b (MSB); and 1989 (MSC)]. In Meehl's model, the origin and why the system is phase locked with the seasonal cycle are not known. How and when the turnabout between trends takes place is not quite clear either. Further study is also needed to clarify the following questions:

1. Why do interannual ENSO modes propagate eastward? Meehl (1987) claimed that the eastward propagation could be simply a local enhancement of the annual cycle. Here, the most pressing need is for an exact determination of the phase relationship between SST, convection, low-level westerlies, and the activity of transient disturbances. Ahead of convection, SST increases as clear sky persists and low-level winds are weaker than normal. The low-level westerly winds tend to become most intense about three months after the occurrence of maximum convective activity. Transient disturbance activity is pronounced in regions of strong westerly winds and convection. Stronger westerlies may contribute to greater heat removal from the ocean surface via stronger heat fluxes, while above normal transient disturbance

activity could cause large upper ocean mixing. Hence, SST cannot be maximum in regions of maximum convection and anomalous westerlies. In general, the highest SST occurs to the east of active convective regions. This favors the eastward propagation of ENSO modes across oceanic regions. Refer to Section 4 for further elaboration on the phase relationship between SST, convection, low-level westerlies, and equatorial disturbance activity on interannual time scales.

2. What are the exact processes through which equatorial intraseasonal perturbations contribute to the ENSO cycle? Does the activity of intraseasonal perturbations indicate any signal of QBO-type interannual variations? These questions should be answered in the present study.

2. Data

The data as well as the computational procedures are the same ones applied in MSA, however for the convenience of the reader, the symbols and computational procedures will be explained once again. To begin with, the three-month running mean values for OLR, SST, and 850 mb u, and 850 mb v are computed.[3] For example, the three-month running mean u at month i which is signified by $\langle u \rangle_i$, is computed by

$$\langle u \rangle_i = 0.25\bar{u}_{i-1} + 0.5\bar{u}_i + 0.25\bar{u}_{i+1} \quad , (1)$$

where an overbar $(\bar{})_i$ represents the monthly mean value at month i. The normal annual cycle (denoted as u_n) was determined from the monthly mean $\bar{u}$ value for each month of the year over all years.

---

[3] Hereafter no mention will be made of the 850 mb level, it will be assumed that all references to wind data (u, v) are at this level unless stated otherwise.

This normal annual cycle was then removed from $\langle u \rangle_i$ to obtain the interannual component (signified as u") as follows:

$$u'' = \langle u \rangle_i - u_n \quad . \quad (2)$$

Thus, u" includes not only interannual variations with periods longer than one year, but also intra-annual perturbations with periods between three months and one year. Similarly, the interannual components v", and OLR", and T_*'' are computed. For brevity, (u", v", OLR", T_*'') perturbations will hereafter be referred to as ENSO modes.

The daily transient component u' is obtained by removing the 6-year (1980-85) mean and the normal annual cycle from the daily u. A band-pass filter procedure is then applied to the transient u' time series, thus further separating the u' data into three frequency bands denoted as u_L (30-60 day), u_M (7-20 day), and u_S (2-6 day) filtered data, respectively. Likewise these groupings are also applied to the transient v' and OLR' values. In this paper, (u_L, v_L, OLR_L) is termed L-mode, (u_M, v_M, and OLR_M) denotes M-mode, and (u_S, v_S, and OLR_S) is defined as S-mode.

Lukas et al. (1984) claimed that "westerly bursts" lasting for about a week over the western Pacific are capable of exciting oceanic Kelvin waves which propagate very quickly eastward (3 m s^{-1}) across the Pacific. In the present study, evidence will be provided that not only (u_L, u_M, u_S) westerly (or easterly) bursts, but also (v_L, v_M, v_S) southerly (or northerly) bursts, as groups, play an important role for the maintenance, as well as the zonal propagation, of ENSO modes. In this regard, the present study concentrates on the total wind field for each mode, i.e., (u_L, v_L) for 30-60 day equatorial disturbances, (u_M, v_M) for 7-20 day equatorial perturbations, and (u_S, v_S) for 2-6 day equatorial disturbances. As mentioned earlier, no correlation exists between these intraseasonal equatorial disturbances and interannual ENSO modes. Nevertheless, there has to be some relationship between the

two modes, therefore we next computed kinetic energy $K_L=(u_L^2 + v_L^2)/2$, $K_M=(u_M^2 + v_M^2)/2$, and $K_S=(u_S^2 + v_S^2)/2$ every day during the six years of 1980-85. The normal annual cycle was determined from K_L, K_M, and K_S values for each day of the year over all years (1980-85). This normal annual cycle was then removed from the 3-month running mean K_L, K_M, K_S values. Interannual components, which are denoted as K_L'', K_M'', K_S'', indicate the amplitude modulation (wave packet) of intraseasonal L-, M-, and S-type equatorial disturbances. Here, the central problem is to examine the relationship between interannual u" modes and the year-to-year variations in (K_L'', K_M'', K_S'') activity.

3. ENSO modes and intraseasonal equatorial disturbances

In Fig. 1, the most important feature is the regular eastward propagation of both u">0 (anomalous westerly) and u"<0 (anomalous easterly) perturbations all the way from the western Indian Ocean to the eastern Pacific. The average phase speed is on the order of 0.3 m s^{-1}, which is approximately 1/10th or less than the speed of the oceanic Kelvin mode. At any fixed geographical location, the ENSO onset (withdrawal) appears to occur in association with the slow eastward propagation of westerly (easterly) u" ENSO modes. In other words, the ENSO onset (withdrawal) is associated with the phase shift from an easterly (westerly) u" phase to a westerly (easterly) u" phase. In Fig. 1, note also the general tendency for a weakening of u" perturbations while crossing over the maritime continent near 100^{o}-120^{o}E. These perturbations intensify when approaching the western Pacific and reach their maxima over the eastern Pacific around 150^{o}-140^{o}W.

There exists a close association of anomalous u" westerlies (easterlies) with above (below) normal convection. Thus, regions of anomalous westerlies (u">0) and above normal convection (OLR"<0) correspond to an updraft portion of the ENSO mode. Conversely,

regions of anomalous easterlies (u"<0) associated with below normal convection (OLR">0) represent a downdraft leg of the ENSO mode. Figure 1 depicts a pronounced QBO-type fluctuation of the equatorial E-W vertical overturning. In March 1982 (pre-ENSO phase), the anomalous vertical overturning is associated with an updraft portion (u">0, OLR"<0) over the western Pacific near 140°E and a downdraft portion (u"<0, OLR">0) covering the eastern Pacific around 140°W. One year later in March 1983 (peak ENSO phase), the vertical overturning becomes reversed with downdrafts near 130°E and updrafts around 140°W. This QBO-type aspect will be further elaborated on in Section 4.

Figure 2 reveals many occasions of systematic eastward propagation of equatorial L-modes across the Indian Ocean and the western Pacific. Typical eastward propagation of westerly u_L perturbations is illustrated by L1, L2, ..., L6. An average eastward phase speed for these westerly u_L perturbations is about 5 m s^{-1}. [v_L perturbations also propagate eastward with the same phase speed (not shown).] At any rate, an inspection of Fig. 2 indicates that individual L-modes do not appear to contribute much to the ENSO onset over the central and eastern Pacific (key area for ENSO). At present, it is not yet known exactly how equatorial L-modes can interact with ENSO modes. The phase speed of L-modes (5 m s^{-1}) is more than one order of magnitude faster than that of ENSO modes (0.3 m s^{-1}). This makes it difficult to further investigate the exact interaction processes between these two different equatorial modes. In Fig. 2, of interest is the tendency of u_L perturbations to intensify during the westerly phase of interannual u" modes, while they tend to weaken during the easterly phase (u"<0). Therefore, it is highly probable that the amplitude (or kinetic energy) variations of intraseasonal u_L perturbations correlate positively with interannual u" modes.

Figure 3 indicates the evolution of 3-month running mean anomaly kinetic energy, i.e., $K_L''=(u_L^2 + v_L^2)''/2$ (thin full lines), as well as the eastward progression of westerly u" perturbations

(heavy full line). Over the central Indian Ocean around 80°E, we see no significant correlation between K_L'' and u". In this vicinity, extraordinarily strong K_L'' activity between April and July 1982 coincides with near zero or slightly negative (easterly) u", while between July and September 1981 moderate K_L'' activity is associated with distinct westerly u" anomalies. Conditions are different over the western Pacific (140°E), where K_L'' is substantially large (1.0 m^2s^{-2}) during the pre-ENSO phase from July to December 1981, and later reaches a maximum (1.5 m^2s^{-2}) when u" westerlies become strongest around March-May 1982 (ENSO peak phase over the western Pacific). This is followed by the drastic reduction in K_L'' after the 1982 summer. Further east between about 160°E and 180°, K_L'' becomes most pronounced about 1 to 3 months after the occurrence of maximum u" westerlies. East of the date line over the eastern Pacific, K_L'' is small, and hence 30-60 day perturbations contribute little to the in situ development of interannual ENSO modes. In short, over the western Pacific between 140°E and 180°, there exists a direct relationship between the frequency of occurrence and the amplitude of equatorial L-type disturbances and u" anomaly fields. In this vicinity, groups of (u_L, v_L) disturbances, as expressed by K_L'', appear to have some association with interannual u" fluctuations over the same region. There is no indication of K_L'' over the Indian Ocean as well as the western Pacific acting as a remote forcing for the enhancement of u" perturbations further downstream (the eastern Pacific).

As mentioned earlier, individual (u_L, v_L) perturbations propagate eastward with a speed of about 5 m s^{-1}. On the other hand, Fig. 3 indicates a very slow eastward phase propagation (~0.3 m s^{-1}) of K_L'' anomalies. In short, the time scale of K_L'' becomes much longer (2 years or longer) than that of individual (u_L, v_L) perturbations (30-60 day). The phase speed of K_L'' anomalies is nearly identical to that of ENSO modes, and hence correlates well with interannual u" perturbations. This indicates that groups of (u_L, v_L) disturbances may possibly interact and supply the energy

needed for the maintenance of ENSO modes. Here, recall that Fig. 3 depicts the evolution of K_L'', i.e., the sum of $(u_L''^2)/2$ and $(v_L''^2)/2$. As shown in Fig. 24 of MSA, the phase propagation of $(u_L''^2)/2$ is very slow (0.3 m s^{-1}) and eastward. Similarly, $(v_L''^2)/2$ also propagates eastward with the same phase speed. Thus, both components are equally important when considering the interaction between L-modes and ENSO modes.

Yet another feature of interest in Fig. 3 is the QBO-type nature of K_L'' variations. This is best exemplified over the central Indian Ocean near 80^o-100^oE. Here, the 1981 summer is characterized by the association of above normal K_L'' with westerly u" anomalies. Similar conditions of above normal K_L'' and westerly u" anomalies occur once again during the 1983 summer. The QBO-type feature is also apparent over the western and eastern Pacific.

Individual (u_M, v_M) equatorial disturbances propagate westward at a speed of about 9 m s^{-1}, but the wave packet of these disturbances (as defined by K_M'') moves very slowly eastward with the same speed as the ENSO modes (refer to Fig. 4). The space scale of (u_M, v_M) disturbances is on the order of 3-4,000 km (Figs. 9, 13, and 17 of MSA), while K_M'' anomaly fields exhibit planetary-scale features of 10,000 km or longer (Fig. 4). Since K_M'' anomalies and ENSO (u", v") modes have the same time and space scales, it is possible that a group of time-clustering and space-overlapping (u_M, v_M) equatorial disturbances can provide the energy for the in situ enhancement (or maintenance) of interannual ENSO modes. [Exactly speaking, the barotropic interaction is related to the sum of products of $u''(\partial u_M u_M/\partial x + \partial u_M v_M/\partial y)''$ and $v''(\partial u_M v_M/\partial x + \partial v_M v_M/\partial y)''$. However, the correlation between u" and K_M'' is an approximate indicator of the barotropic interaction between (u_M, v_M) disturbance groups and ENSO modes.]

It turns out that a distinct zone of large K_S'' tends to propagate eastward from about 180^o on September 1982 to 120^oW in April 1983 (not shown); hence, its phase speed is very slow and nearly identical to that of the westerly u" mode. Even though

individual u_S disturbances generally move westward at a speed of about 15 m s^{-1} (Fig. 23 of MSA), groups of (u_S, v_S) disturbances; i.e., K''_S, propagate very slowly eastward (0.3 m s^{-1}).

To further substantiate interannual variations of the intraseasonal disturbance activity, correlations were computed for K''_L, K''_M, and K''_S using u" as the reference time series at every 5 degrees of longitude along the equator from 50°E to 120°W during the six years of 1980-85. A correlation coefficient greater than 0.41 is significant at the 95% confidence level. The simultaneous (no lag) correlation between u" and K''_L (Fig. 5C) exceeds the 95% confidence level over the western Pacific between about 140°E and the date line, while it is quite small, although positive, over the eastern Pacific where the activity of 30-60 day oscillations is generally weak. In Fig. 5B, simultaneous correlation between u" and K''_M is positive everywhere along the equator from 50°E to 120°W. Of particular interest is a marked band of large correlation in excess of +0.45 from the date line at lag -5 to 0 months (K''_M leading) to 120°W at lag 0 months. This means that the central and eastern Pacific (180°-120°W) are characterized by strong activity of intraseasonal M modes prior to and during the westerly phase of interannual u" modes, perhaps indicating an in situ nonlinear coupling between the two modes over that region, as speculated earlier. The correlation between u" and K''_S is positive over the central and eastern Pacific (Fig. 5A). Thus, (u_S, v_S) equatorial disturbances are also responsible for the enhancement and maintenance of interannual u" modes over the same region. At any rate, the correlation maps shown in Fig. 5 provide useful information pertaining to a phase relationship between u" and (K''_L, K''_M, K''_S). Such a phase relationship is of fundamental importance when determining the structural features of ENSO modes.

4. Monsoons and ENSO

As outlined in Section 1, no external forcing is included in Meehl's (1987) model for ENSO episodes. It includes QBO-type oscillations that internally evolve due to the monsoon activity over the Indian and western Pacific sectors of an ocean-atmosphere coupled system. Figure 6 demonstrates the annual cycle of u_n (normal zonal winds as defined in eq. 2) along the equator. In July u_n westerlies, which reflect the monsoon activity over the Indian subcontinent and Southeast Asia, are nearly stationary until October. Between November and December, the u_n westerlies extend eastward and cover the eastern Indian Ocean-maritime continent-western Pacific region from about 90^{o} to 160^{o}E. This corresponds to the eastward traverse of monsoon westerlies from northern summer to southern summer. In January, monsoon westerlies are strongest not at the equator, but at about 5^{o}-10^{o}S between 100^{o} and 160^{o}E. After January, the equatorial monsoon westerlies tend to retreat westward to the Indian Ocean. However, the westward return excursion from January to April is not well defined. By April, the monsoon westerlies are re-established over the central Indian Ocean near 80^{o}-90^{o}E.

Figure 7 shows the evolution of 3-month running mean <u>, i.e., u_n + u" as defined in eq. (2), along the equator. The 1981 summer corresponds to a "strong monsoon" over the Indian region, since <u> westerlies are stronger than normal u_n. Regions of above normal westerlies (u">0) then move eastward following a nearly identical trajectory as that of u_n westerlies (see Fig. 6). By January 1982, above normal westerlies reach the western Pacific (130^{o}-150^{o}E) where the Southern Hemisphere summer monsoon becomes more active than usual. At this time, <u> easterlies over the eastern Pacific are also stronger than usual, i.e., u"<0 (also see Fig. 1). This implies an unusual intensification of the Walker Circulation over the Pacific. Regions of above normal <u> westerlies move further eastward, reaching the central Pacific near 170^{o}E-180^{o} by July 1982. This corresponds to the ENSO onset over the central Pacific. Simultaneously, the <u> easterlies near the

western end of the Indian Ocean become unusually strong; i.e., u"<0, implying a "weak monsoon" during the 1982 summer. Regions of "weak monsoon" then shift eastward, as shown by the heavy dashed lines in Figs. 1 and 7. Also note that <u> westerlies near 100°E in November and December 1982 are extraordinarily weaker than normal u_n. It is a great surprise to see the prevalence of <u> easterlies over the western Pacific around 150°E in January 1983. Thus, the Southern Hemisphere summer monsoon is exceptionally weak during the 1982-83 southern summer as compared with the "strong Southern Hemisphere monsoon" of one year earlier, i.e., the 1981-82 southern summer. Such an alternation of monsoon activity from one year to another can also be seen over the Indian Ocean. We see the re-establishment of unusually strong <u> westerlies (or u">0) over the central Indian Ocean in July 1983. Recall that similar "strong monsoon" conditions are encountered two years before, i.e., July 1981. Thus, Fig. 7 clearly indicates the biennial nature of monsoon activity over the Indian Ocean as well as the Pacific region. The 1982-83 ENSO over the central and eastern Pacific occurs as a result of a modulation of the annual (or monsoon) cycle. It also appears in Fig. 7 that the birthplace of ENSO modes is the western Indian Ocean, in agreement with the findings by Barnett (1983) and Yasunari (1987).

A fundamental question still remains unanswered. Why ENSO modes propagate very slowly eastward all the way from the Indian Ocean to the eastern Pacific. Here, the pressing need is to investigate the exact phase relationship between u", OLR", T_*'', and (K_L'', K_M'', K_S''). The correlation map of Fig. 5 illustrates that interannual disturbance activity (K_L'', K_M'', K_S'') becomes most pronounced at nearly the same time as, or one to two months prior to, the occurrence of maximum u" westerlies. OLR" becomes minimum (most pronounced convective activity) about 3 months after the highest T_*'' anomaly over most of the Indian Ocean and the Pacific (MSB, 1988). Figure 8 exemplifies the phase relationship between OLR" and u". Namely, the u" westerly maximum is located about 2-

4,000 km west of the OLR" minimum. (Since the eastward phase speed of ENSO modes is about 0.3 m s^{-1}, this distance roughly corresponds to a 2-3 month lag.) In Fig. 8, T_*'' was determined over 4^o longitude by 4^o latitude resolution boxes with at least one or more T_* observations in each month throughout the six years of 1980-85. This criterion was not met over the central Pacific between about 165^oE to 170^oW, and thus no attempt was made to evaluate T_*'' over that region. At any rate, Fig. 8 presents evidence that T_*'' data thus determined are adequate, at least qualitatively, to describe the phase relationship between T_*'' and other parameters, such as u" and OLR". In Fig. 8c for October 1982, T_*'' is positive and substantial (3^o-4^oC) over the eastern Pacific around 160^o-140^oW. With reference to this T_*'' maximum, OLR" becomes minimum near 170^oW, i.e., 20^o-30^o longitude westward of the T_*'' maximum. The u" westerly maximum occurs about 30^o-40^o longitude west of the T_*'' maximum. The presence of highest T_*'' ahead of minimum OLR" and maximum u" favors the eastward phase propagation of ENSO modes. A similar phase relationship between T_*'', OLR", and u" can also be found in Figs. 8a and b. Here, note that all diagrams of 8a to 8c are for the transition period, either for April or October, when monsoon activity becomes the least pronounced. Hence, Fig. 8 probably indicates the structure of ENSO modes themselves, and does not reflect the monsoon structure.

Combining all the information obtained in the present study, together with the findings in MSA and MSB, I would like to propose a tentative model establishing the relationship between interannual T_*'', OLR", and u" variations as shown in Fig. 9 where highest T_*'' anomalies occur about 2-4 months ahead of the eastward propagating OLR" and u" perturbations. Note that this lag is very short when one considers the time scale (2 years or longer) of interannual variations. The model proposed in Fig. 9 is valid for interannual modes occurring over an extensive region covering both the Indian and Pacific Oceans. Here, a question arises. What are the major factors that determine the intensity and location of oceanic T_*''

anomalies relative to atmospheric OLR" and u" perturbations? As emphasized many times before, intraseasonal disturbance activity (K''_L, K''_M, K''_S) may exert some measure of control upon determining sea surface temperature on interannual time scales. The heat removal from the ocean surface is proportional to the low-level wind speed, i.e., $u_n + u''$. The normal u_n profile along the equator (Fig. 6) is largely determined by monsoon activity in both hemispheres. When u" westerly perturbations pass through regions of u_n westerlies, the heat removal from the ocean surface becomes larger than normal, thus contributing to the decrease in T''_*. Conversely, when u" westerlies reach the central and eastern Pacific where strong trade winds ($u_n<0$) prevail, SST over that region tends to become higher than normal because of the reduction in heat fluxes from the ocean surface. Thus, monsoon activity in both hemispheres plays an important role in determining the T''_* fields along the equator. Lau and Shen (1988) claimed that the zonal advection of normal sea surface temperature (T_{*n}) is primarily responsible for the intensification and eastward propagation of ENSO modes over the western Pacific. However, over the Indian Ocean where the zonal gradient of T_{*n} is near zero, ENSO modes must owe their existence to other factors, rather than the zonal T_{*n} advection effect. One also should not overlook the importance of radiational effects on interannual time scales. These effects as outlined above require further clarification and elaboration.

(1) Disturbance (DIS) effects

Individual (u_L, v_L) wind speeds are on the order of 2-4 m s^{-1} over the Indian Ocean and the western Pacific (Fig. 2). In comparison, both (u_M, v_M) and (u_S, v_S) equatorial disturbances are pronounced over the entire Pacific with an average wind speed of about 3-5 m s^{-1} (Figs. 22 and 23 of MSA; refer also to Fig. 5 of this paper). Of course, these equatorial intraseasonal disturbances are much less intense as compared with tropical depressions developing away from the equator. In general, SST tends to decrease by several degrees when tropical depressions

approach. On interannual time scales, a measure of disturbance activity is expressed as K_L'', K_M'', and K_S'', which are all on the order of 1 to 2 m^2s^{-2}. Thus, the sum of K_L'', K_M'', and K_S'' occasionally exceeds 3-5 m^2s^{-2}. This value is quite large when considering that it is for 3-month running mean anomalies. In Fig. 9, regions of strong intraseasonal disturbance activity K_L'', K_M'', and K_S'' are schematically shown by waves at the sea surface. Our contention is that groups of intraseasonal disturbances may contribute to an increase in upper ocean mixing, eventually resulting in a decrease in T_*''. These disturbance effects, which are signified as DIS, appear to be important in determining the T_*'' perturbations relative to u" and/or OLR" anomalies. In particular, the eastward propagating ENSO modes over the Indian Ocean owe their existence to DIS effects. Judging from the correlation maps in Fig. 5, as well as from the correlation between OLR" and T_*'' depicted in Fig. 10 of MSB; T_*'' should decrease quickly before the arrival of above normal convective regions (OLR"<0) and continue to be below normal several months after the passage of anomalous westerly zones (u">0).

(2) Monsoon (MON) effects

An approximate heat flux from the sea surface on interannual time scales is proportional to the 3-month mean zonal wind speed, i.e., $\langle u \rangle = u_n + u''$. This value has to be compared with the normal zonal wind speed u_n along the equator, which reflects the monsoonal circulation in both hemispheres. We then compute the difference between the two values as follows:

$$DU = |u_n| - |u_n + u''| \quad . \quad (3)$$

DU is an index for monsoon effects (denoted as MON) upon interannual T_*'' variations. In January 1982 (pre-ENSO phase) over the eastern Pacific (150°-120°W), the trade winds are stronger than normal by more than 2 m s^{-1} (Figs. 6 and 7), and DU becomes negative and substantial. Perhaps, this results in below normal

T_*'' (<0) due to an excess heat flux from the sea surface. Conversely, the mature phase of ENSO (January 1983) is characterized by large positive DU and well above normal T_*'' (>0), since the strong normal trade winds (u_n<0) are replaced by weak westerlies (<u> = u_n + u" > 0). In general, ENSO modes tend to weaken while passing over the eastern Pacific. This weakening appears to be largely due to MON effects. To the east of above normal convection (OLR"<0), both u_n and u" are easterly, consequently T_*'' tends to become negative due to negative DU, while west of OLR"<0, positive DU tends to induce positive T_*''. Hence, MON effects are not favorable for the eastward propagation of ENSO modes over the eastern Pacific. Moreover, MON effects even contribute to the damping of ENSO modes in this vicinity. The situation is different over the western Pacific where u_n is westerly. Here, MON effects are one of the important contributors to the intensification and eastward propagation of ENSO modes. Unfortunately, MON effects have not been included in any of the atmosphere-ocean coupled numerical ENSO models thus far proposed.

The interannual variations in zonal winds, i.e., <u> = u_n + u", are important indicators for changes in upwelling (or downwelling) on interannual time scales. Over the eastern Pacific, for example, u" easterlies in January 1982 may induce stronger than usual upwelling and negative T_*'', while u" westerlies in January 1983 are an indicator of unusually weak upwelling, or even downwelling, and positive T_*''.

(3) Advection (ADV) effects

Assuming that the ocean currents are proportional to the low-level winds on interannual time scales, the zonal advection of sea surface temperature on interannual time scales can be approximated as

$$-(u\frac{\partial T_*}{\partial x})'' = \left((u_n + u'' + u')\frac{\partial T_{*n} + T_*'' + T_*'}{\partial x}\right)''$$

$$= -u_n\frac{\partial T_*''}{\partial x} - u''\frac{\partial T_{*n}}{\partial x} - \left(u''\frac{\partial T_*''}{\partial x} - \left\langle u''\frac{\partial T_*''}{\partial x}\right\rangle\right) - \left(u'\frac{\partial T_*'}{\partial x}\right)'' \quad , \quad (4)$$

where the notation ( )' refers to quantities with intraseasonal time scales shorter than about 60 days. The last term of eq. (4) represents interannual T_*'' changes due to the zonal advection of intraseasonal T_*' perturbations via intraseasonal u' oceanic currents. This advection effect is probably not significant, since oceanic u' responses, as well as T_*' perturbations, on intraseasonal time scales are assumed to be quite small. Recall that DIS effects discussed earlier have nothing to do with the horizontal T_*' advection due to intraseasonal motions.

The third term of eq. (4) indicates the advection (anomaly) of T_*'' perturbations due to interannual u" currents. If u" and T_*'' at i month are both nearly the same as those in i-1 and i+1 months, then the difference between $u''\partial T_*''/\partial x$ at i month and the 3-month mean $\langle u''\partial T_*''/\partial x\rangle$ at i month is close to zero, i.e., $(u''\partial T_*''/\partial x)'' \sim 0$.

The normal T_{*n} is highest (29.5°C) near 150°E at the equator with a large negative gradient ($\partial T_{*n}/\partial x<0$) over the central and eastern Pacific. Over the western Pacific west of 150°E, as well as over the Indian Ocean, the T_{*n} gradient is near zero or slightly positive. The second term of eq. (4) represents the zonal advection of T_{*n} by u" anomaly currents. This advection effect appears to be responsible for the intensification of eastward propagating modes over the central Pacific (Lau and Shen, 1988). However, $u''\partial T_{*n}/\partial x$ is insignificant over the Indian Ocean and the western Pacific, and hence is not capable of explaining the existence of eastward propagating ENSO modes over those oceanic regions.

The first term in eq. (4) contributes to the eastward advection of T_*'' perturbations due to persistent u_n westerlies (Fig. 6) over the central Indian Ocean throughout the year. Between November and January over the western Pacific, u_n westerlies are also substantial and favor the eastward T_*'' advection there. In contrast, east of the date line where u_n is predominately easterly

(Fig. 6), the contribution due to $u_n \partial T_*''/\partial x$ advection is westward. This contradicts the observed eastward progression of T_*'' perturbations across the eastern Pacific (refer to Fig. 9 of MSB and Fig. 8 of this paper). As mentioned earlier, both DIS and MON effects contribute to the eastward progression of T_*'' fields over the eastern Pacific.

For convenience in subsequent discussions, equation (4) can be rewritten as

$$ADV = ADN + ADE \quad , \quad (5)$$

where ADV represents the total advection effect $-(u\, \partial T_*/\partial x)''$, ADN the first advection term in eq. (4), and ADE the second advection term in eq. (4).

(4) Radiational (RAD) effects

Radiational effects (designated as RAD) appear to be one of the major components for the maintenance of T_*'' fields. Let us consider only the incoming solar energy (insolation) at the sea surface. In regions of fine weather (OLR">0), there is a tendency for T_*'' anomaly to become positive. Such a tendency persists until OLR" changes its sign from positive to negative. It is, therefore, expected that the highest T_*'' anomaly occurs ahead (or east) of active convective regions of OLR"<0 (see Fig. 8).

So much for discussions on the major physical processes that are responsible for interannual T_*'' variations. However, many of the fundamental questions concerning the nature and causes of climate T_*'' changes are still largely unsolved because of our incomplete quantitative understanding of these basic processes. Here, it may be worth presenting additional information, although qualitative, on DIS and MON effects in Fig. 10. Comparing this diagram with Fig. 8, one fines that (1) regions of large K_L'' activity approximately coincide with regions of strong u" westerlies, while large positive K_M'' activity tends to occur in the neighborhood of abnormally pronounced convection (OLR" minimum),

and (2) K_S'' is much smaller in its magnitude as compared with K_L'' and K_M''. In fact, K_M'' is largest, indicating the most importance of M-type (7-20 day) equatorial disturbances upon the maintenance, via DIS effects, of interannual T_*'' variations. Of course, L-type (30-60 day) equatorial disturbances are also important.

Characteristics of T_*'' perturbations and associated physical processes in October 1982, which can be diagnosed from an inspection of Figs. 8c and 10c, are summarized in Table 1. In this table the signs of various physical processes are indicated for vertical columns located at regions of (a) large positive T_*'' (160^oW-140^oW), (b) near zero T_*'' (150^oE-170^oW), and (c) positive T_*'' (70^oE-100^oE). For example, the term "near zero" for DIS over region a indicates a tendency for T_*'' perturbations to stay near normal due to this particular effect over the eastern Pacific. In this vicinity, (K_L'', K_M'', K_S'') are all quite small in October 1982 (Fig. 10c), and thus DIS effects are insignificant. In Table 1 for region a, MON effects contribute largely to increase T_*'' anomalies, because of the reduction in heat fluxes from the sea surface (DU>>0), as well as the weakening of upwelling (u">0). The contribution due to ADV advections, in particular due to ADE advection (eq. 5) is also important for anomalously high T_*'' over region a. RAD effects appear to be relatively small. In short, MON and ADV are two of the most important physical processes which are responsible for high T_*'' anomalies over region a (eastern Pacific) in October 1982 (mature phase of 1982-83 ENSO).

Over region b (central Pacific), large positive ADV effects are nearly compensated for by large negative DIS effects. This results in very small, although positive, T_*'' anomalies over region b, which is dominated by prominent u" westerlies and above normal convection (OLR"<0). Also, large negative DU effects are perhaps overcompensated for by positive downwelling effects due to strong westerly u" anomalies (Fig. 1). Over region c (Indian Ocean), ADV effects are much less important than DIS and MON effects. The latter two effects are both positive and substantial to induce

positive T_*'' perturbations over the Indian Ocean.

Similar diagnoses were also performed for October 1981 using Figs. 8a and 10a, as well as for April 1982 utilizing Figs. 8b and 10b. For brevity, however, the diagnostic results are not reproduced here. There exists significant regional differences in the relative importance of basic physical processes. No single physical process can explain T_*'' anomalies over all the oceanic sectors extending from the Indian Ocean to the eastern Pacific. In addition, the relative importance of physical processes differs substantially with different phases of the ENSO cycle.

As pointed out by Murakami (1988), 30-60 day T_{*L} perturbations exhibit eastward phase propagation. An inspection of Figs. 2 and 7 indicates the systematic eastward propagation of u_L perturbations in regions of 3-month mean westerlies, i.e., $\langle u \rangle = u_n + u'' > 0$. This can be explained as follows: Referring to eqs. 4 and 5, ADN and ADE effects on 30-60 day time scales can be expressed as

$$\mathrm{ADN} = -(u_n + u'')\frac{\partial T_{*L}}{\partial x} \quad ,$$

$$\mathrm{ADE} = -u_L\frac{\partial T_{*n} + \partial T_*''}{\partial x} \quad .$$

It is immediately apparent that ADN represents eastward advection of T_{*L} perturbations when and where 3-month mean (u_n + u") winds are westerlies. This favors the eastward propagation of T_{*L} perturbations. Conversely, when (u_n + u") winds are easterly (for example, over the eastern Pacific in October 1981), L modes tend to propagate westward (Fig. 2). The magnitude of T_*'' perturbations is on the order of 0.5°C (see Fig. 3 of Murakami, 1988). In comparison, u_L in ADE which represents the response in 30-60 day oceanic currents, is probably quite small because of the short time scales in question. As such, ADE is expected to be much less important when compared with ADN. DIS effects on 30-60 day time scales are related to the association of u_L with K_M and K_S.

Similar to Fig. 5, we also evaluated the correlation between u_L and $(K_M, K_S)_L$. The correlation is positive and statistically significant (not shown), implying that K_M and K_S activity becomes more (less) active than normal when and where u_L is westerly (easterly). In short, ADN and DIS are probably the leading effects in determining the phase relationship of T_{*L} anomalies with reference to u_L and OLR_L perturbations. At present, how important are MON and RAD effects on 30-60 day time scales is not immediately obvious. Further study is needed.

5. Concluding remarks

Data utilized in this study are ECMWF 850 mb winds, outgoing longwave radiation (OLR), and sea surface temperature (T_*) during the six years of 1980-85. Some of the characteristic features of ENSO modes are described in terms of three-month running mean anomalies, which are signified as u", v", OLR", and T_*'', respectively. Daily OLR and 850 mb winds are subjected to a band-pass filter to obtain climatological information on equatorial disturbances. These filtered data are denoted as u_L, v_L, and OLR_L (30-60 day); u_M, v_M, and OLR_M (7-20 day); and u_S, v_S, and OLR_S (2-6 day), respectively. These intraseasonal L-, M-, and S-modes are clearly separate from interannual ENSO modes.

The main objective is to investigate the mutual relationship among atmospheric (u", v", and OLR") ENSO modes, intraseasonal disturbance activity (K_L'', K_M'', K_S''), and oceanic T_*'' variations. To the west (~5,000 km) of highest T_*'' anomalies, the strongest u" westerlies are located. Situated between these T_*'' anomalies and u" westerlies, is encountered the lowest OLR" (above normal convection) center. More specifically, it is situated approximately 3,000 km west of the T_*'' maximum. There exists significant regional difference in basic physical processes that are responsible for determining the relative phase difference among

T_*'', OLR", and u". No single physical process can explain (T_*'', OLR", u") perturbations over the different oceanic sectors ranging from the Indian Ocean to the eastern Pacific. The relative importance of physical processes also differs with each phase of ENSO; namely, where and when these eastward propagating interannual modes are passing through. Basic physical processes are as follows:

(1) Radiational (RAD) effects

There exists strong incoming solar energy in regions of fine weather (OLR">0), that contributes to an increase in T_*'' anomaly. Accordingly, the highest T_*'' anomaly tends to occur ahead (or east) of active convective regions of OLR"<0. RAD effects on interannual time scales appear to be one of the major components for the maintenance of T_*'' fields over all oceanic sectors.

(2) Disturbance (DIS) effects

T_*'' tends to become below normal in regions of strong intraseasonal disturbance activity; i.e., $K_L''>0$, $K_M''>0$, and $K_S''>0$, due to their upper ocean mixing. The Indian Ocean is characterized by prominent K_L'' and K_M'' activities (Figs. 3-5). ENSO modes over the Indian Ocean, although relatively weak as evident in Fig. 1, primarily owe their existence to DIS as well as RAD effects. Over the western Pacific, all types of intraseasonal disturbance activity (K_L'', K_M'', K_S'') are pronounced and contribute to the eastward propagation of ENSO modes. In comparison, K_L'' activity becomes insignificant when ENSO modes approach the eastern Pacific.

(3) Monsoon (MON) effects

As defined in eq. (3), DU is introduced as an index for monsoon (MON) effects. The heat removal from the sea surface on interannual time scales is supposed to be below normal when and where DU becomes positive, resulting in positive T_*'' anomaly, while the reverse is true if DU is negative. MON effects appear to be most important over the central and eastern Pacific, where positive DU always occurs in conjunction with and to the east of the westerly u" maximum. (For brevity, the longitude-time section of

DU is not reproduced here.) Conversely, DU is negative to the west of the westerly u" center. This favors the development, as well as the eastward propagation of ENSO u" perturbations. MON effects are also substantial over the Indian Ocean.

In Fig. 1, we see large interannual changes in u" occurring over the central and eastern Pacific. This is an indication of pronounced interannual variation of upwelling in this particular oceanic sector. In January 1982 (pre-ENSO phase), u" is easterly, indicating upwelling stronger than usual and T_*'' anomaly below normal. Conversely in January 1983 (mature ENSO phase), prominent u" westerlies are probably associated with well below normal upwelling and above normal T_*''.

(4) Advection (ADV) effects

As defined in eq. (5), ADN represents the zonal advection of T_*'' perturbations due to normal (or monsoonal) u_n winds, while ADE determines the zonal advection of normal T_{*n} fields via interannual u" perturbations. ADN contributes to the eastward advection of T_*'' due to prevailing u_n westerlies (Fig. 6) over the Indian Ocean. Thus, ADN effects are one of the most important processes for the existence of eastward propagating ENSO modes over the Indian Ocean. East of the date line over the eastern Pacific, u_n is predominantly easterly and the contribution due to ADN is westward. This westward advection is unfavorable for the eastward propagation of ENSO modes. In contrast, ADE contributes greatly to the eastward propagation of ENSO modes across the eastern Pacific, where the normal SST gradient; i.e., $T_{*n}/\ x$, is negative and substantial. ADE effects are also important over the central Pacific.

The foregoing discussion is admittedly somewhat speculative. Further studies are certainly needed for an quantitative (not qualitative) measurement of each physical process. It is also imperative to introduce appropriate ocean-atmosphere coupled numerical models to test various physical processes involved in ENSO modes.

Acknowledgments

The author is indebted to Mrs. Dixie Zee for her assistance in data processing and final editing of this manuscript.

This research has been supported by the National Science Foundation under Grant ATM 86-09968.

APPENDIX

List of Acronyms and Symbols

OLR	outgoing longwave radiation
SST	T_*; sea surface temperature
ENSO	El Nino/Southern Oscillation
ECMWF	European Centre for Medium Range Weather Forcasts
$(\ )''$	3-month running mean anomaly data
$(\ )_n$	normal annual cycle
$(\ )_S$	2-6 day filtered data
$(\ )_M$	7-20 day filtered data
$(\ )_L$	30-60 day filtered data
S mode	(u_S, v_S, OLR_S) fields
M mode	(u_M, v_M, OLR_M) fields
L mode	(u_L, v_L, OLR_L) fields
K_S	$(u_S^2 + v_S^2)/2$
K_M	$(u_M^2 + v_M^2)/2$
K_L	$(u_L^2 + v_L^2)/2$

K_S''	3-month running mean anomaly K_S
K_M''	3-month running mean anomaly K_M
K_L''	3-month running mean anomaly K_L
DIS	disturbance effects
MON	monsoon effects
ADV	advection effects
RAD	radiational effects
$(\overline{\ \ })$	monthly mean
$\lvert\ \ \rvert$	absolute value
$<\ \ >$	3-month running mean

References

Lau, K.-M., and S.H. Shen, 1988: On the dynamics of intraseasonal oscillation and ENSO. J. Atmos. Sci., 45, 1781-1797.

Lukas, R., S.P. Hayes and K. Wyrtki, 1984: Equatorial sea level response during the 1982-83 El Nino. J. Geophys. Res., 89, 10425-10430.

Meehl, G.A., 1987: The annual cycle and interannual variability in the tropical Pacific and Indian Ocean regions. Mon. Wea. Rev., 115, 27-50.

Murakami, T., 1988: Relationship between sea surface temperature and outgoing longwave radiation on intraseasonal time scales. Tenki, J. Meteor. Soc. Japan, 35, 715-722.

_____, and W.L. Sumathipala, 1988a: Equatorward surges, equatorial westerlies and convection on interannual and intraseasonal time scales. UHMET88-02, Department of Meteorology, University of Hawaii, Honolulu, Hawaii, U.S.A.

_____, 1988b: Relationship between outgoing longwave radiation and sea surface temperature on interannual time scales. UHMET88-03, Department of Meteorology, University of Hawaii, Honolulu, Hawaii, U.S.A.

_____, 1989: Westerly bursts during the 1982/83 ENSO. J. Climate, 2, 71-85.

Yasunari, T., 1987: Global structure of the El Nino/Southern Oscillation. Part I: El Nino composites. J. Meteor. Soc. Japan, 65, 67-98.

_____, 1988: Global teleconnections associated with the Asian monsoon and the ENSO. Jacob Bjerknes Symposium on Air-Sea Interaction, February 1-5, 1988, Anaheim, California.

Table 1. Characteristics of T''_* perturbations and associated physical processes in October 1982

Physical processes	a(160^oW-140^oW) large positive T''_*	b(150^oE-170^oW) near zero T''_*	c(70^oE-100^oE) positive T''_*
DIS	near zero ($K''_L, K''_M, K''_S \sim 0$)	large negative ($K''_L, K''_M >> 0$)	positive ($K''_L, K''_M < 0$)
MON	large positive (DU >> 0) (reduced upwelling)	small positive (DU << 0) (downwelling)	positive (DU > 0)
ADV	large positive (ADN > 0) (ADE >> 0)	large positive (ADN ~ 0) (ADE >> 0)	small positive (ADN ~ 0) (ADE > 0)
RAD	small negative (OLR" < 0)	negative (OLR" < 0)	near zero (OLR" ~ 0)

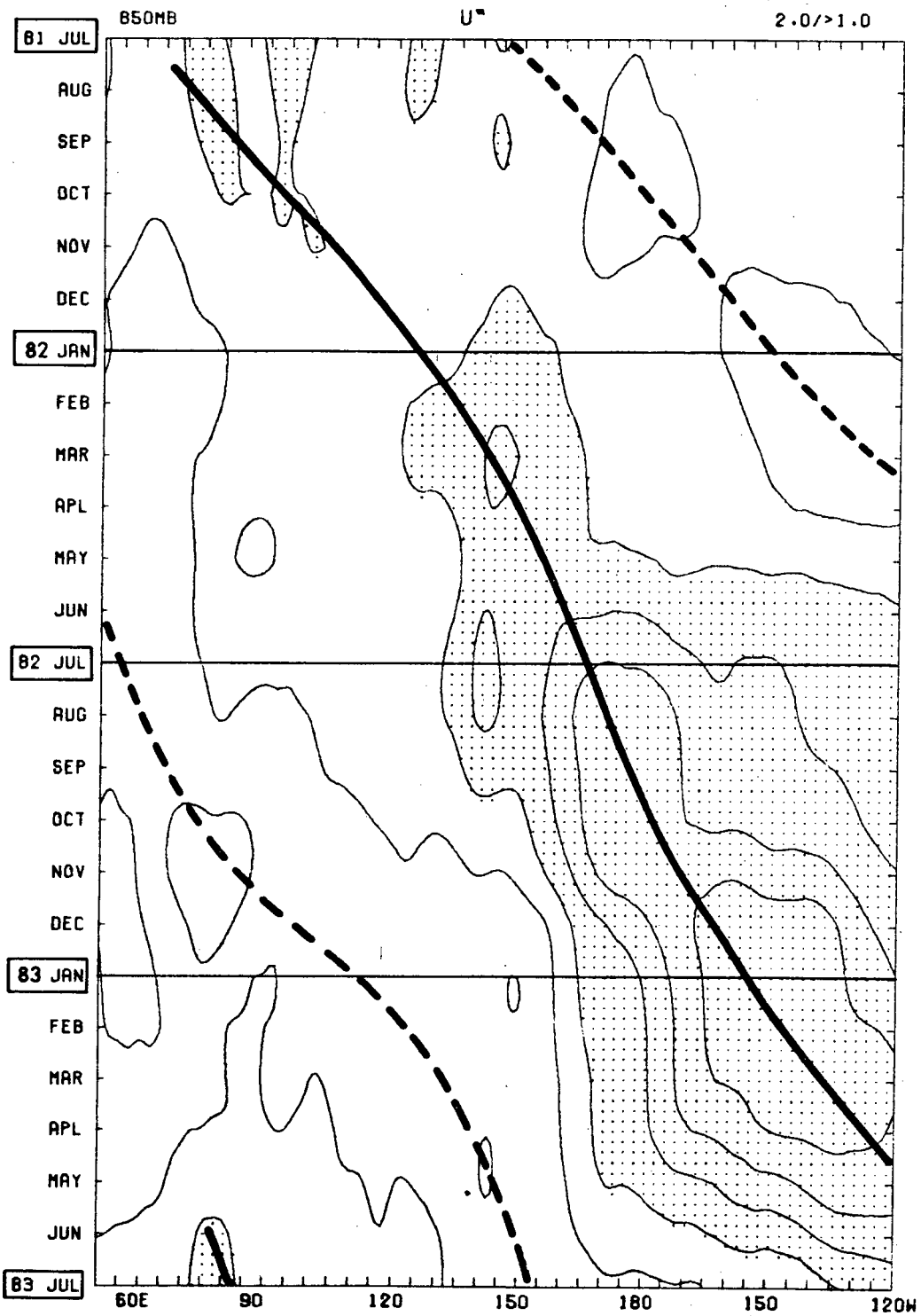

Fig. 1. 850 mb u" (interval: 2 m s^{-1}) at the equator. Shading indicates regions of westerly u" greater than +1 m s^{-1}. Heavy (dashed) lines indicate eastward propagation of westerly (easterly) u".

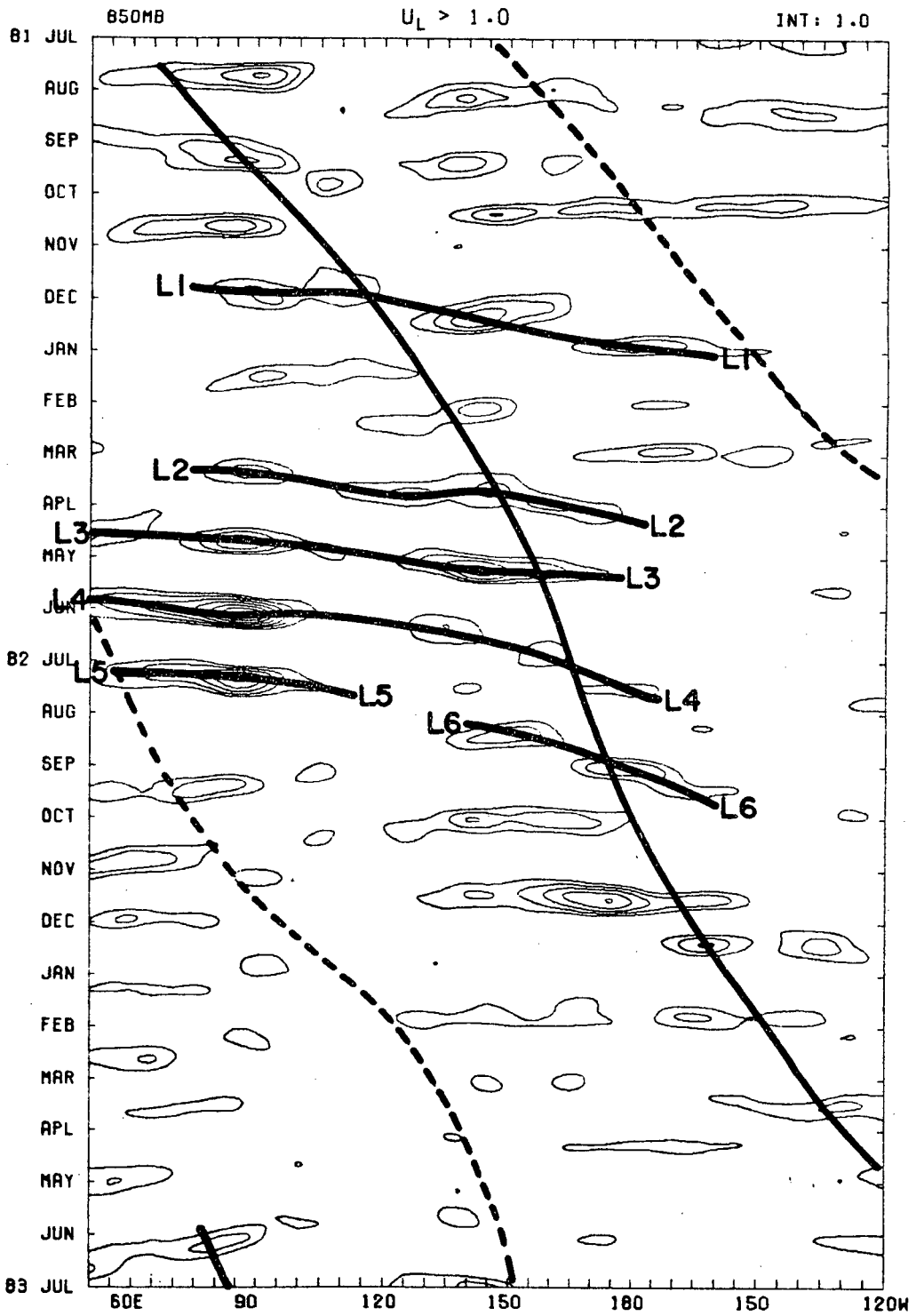

Fig. 2. Longitude-time section of positive (westerly) u_L perturbations greater than +1 m s^{-1}. Intervals are for 1 m s^{-1} (no zero and/or negative isolines). Major eastward propagating perturbations are shown by "L1", "L2", ..., and "L6".

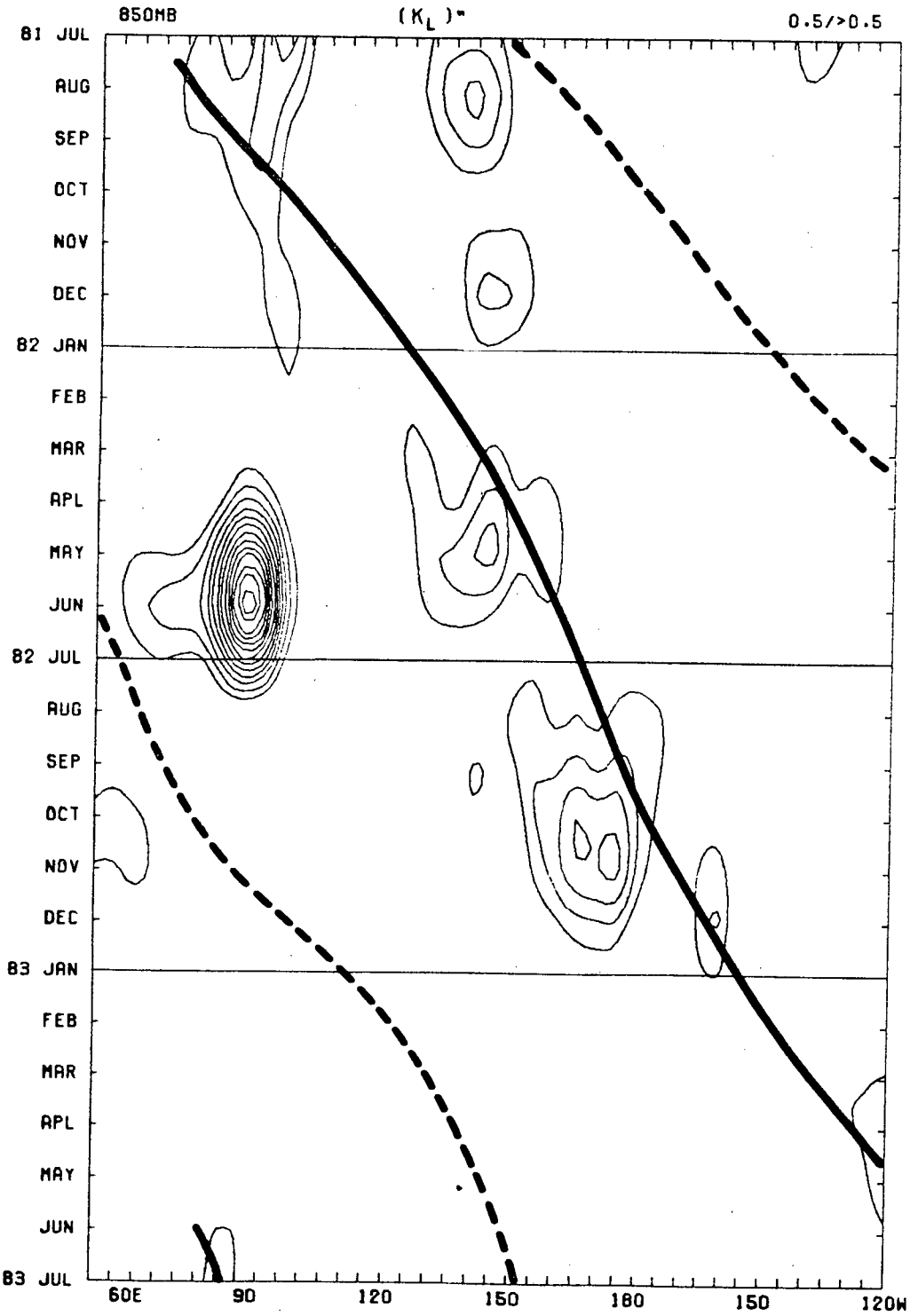

Fig. 3. Longitude-time section of K_L'' anomalies greater than +0.5 $m^2\ s^{-2}$ (interval 0.5 $m^2\ s^{-2}$). Heavy full lines indicate eastward propagation of westerly u" perturbations (see Fig. 1).

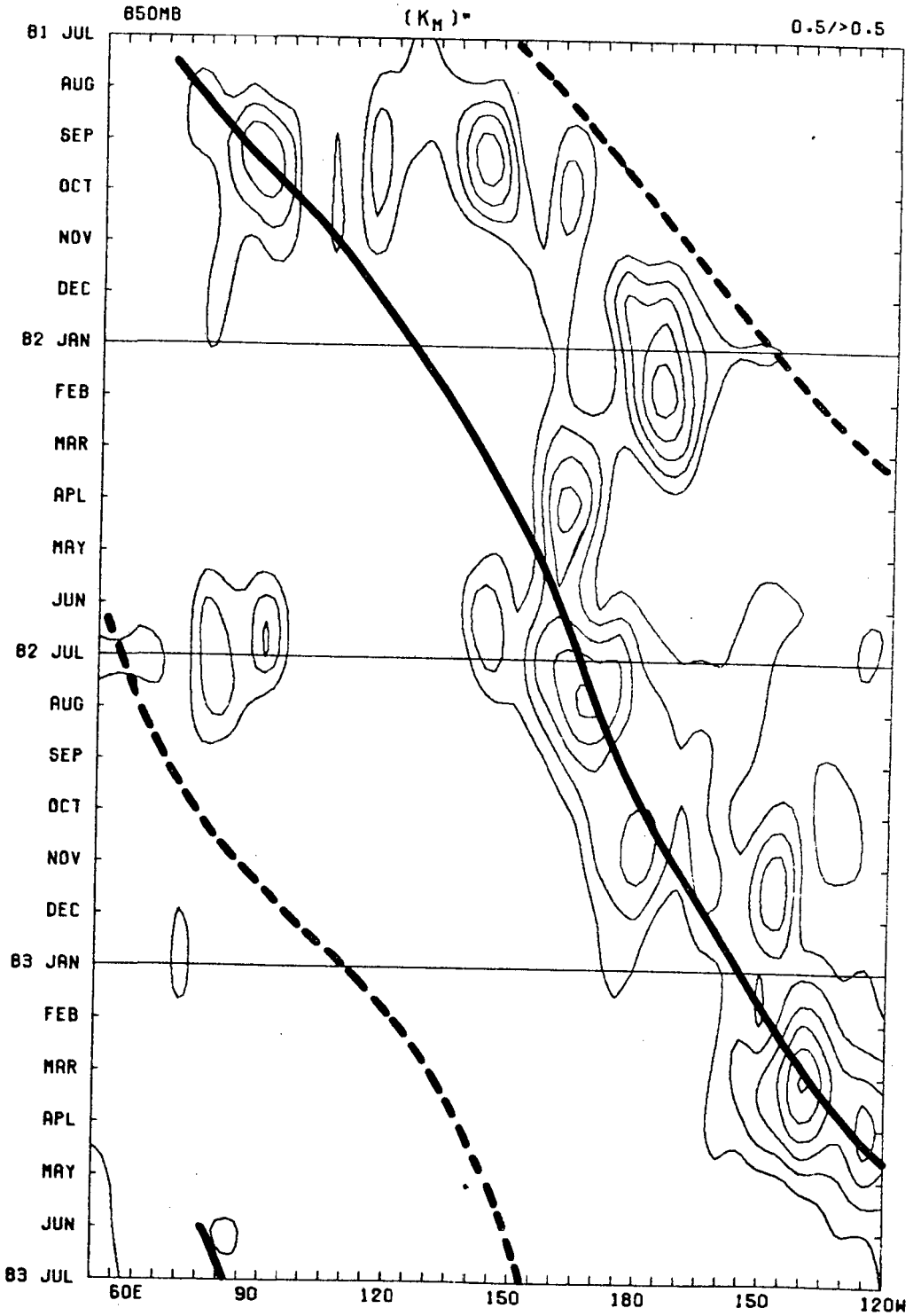

Fig. 4. As in Fig. 3, except for K_M''.

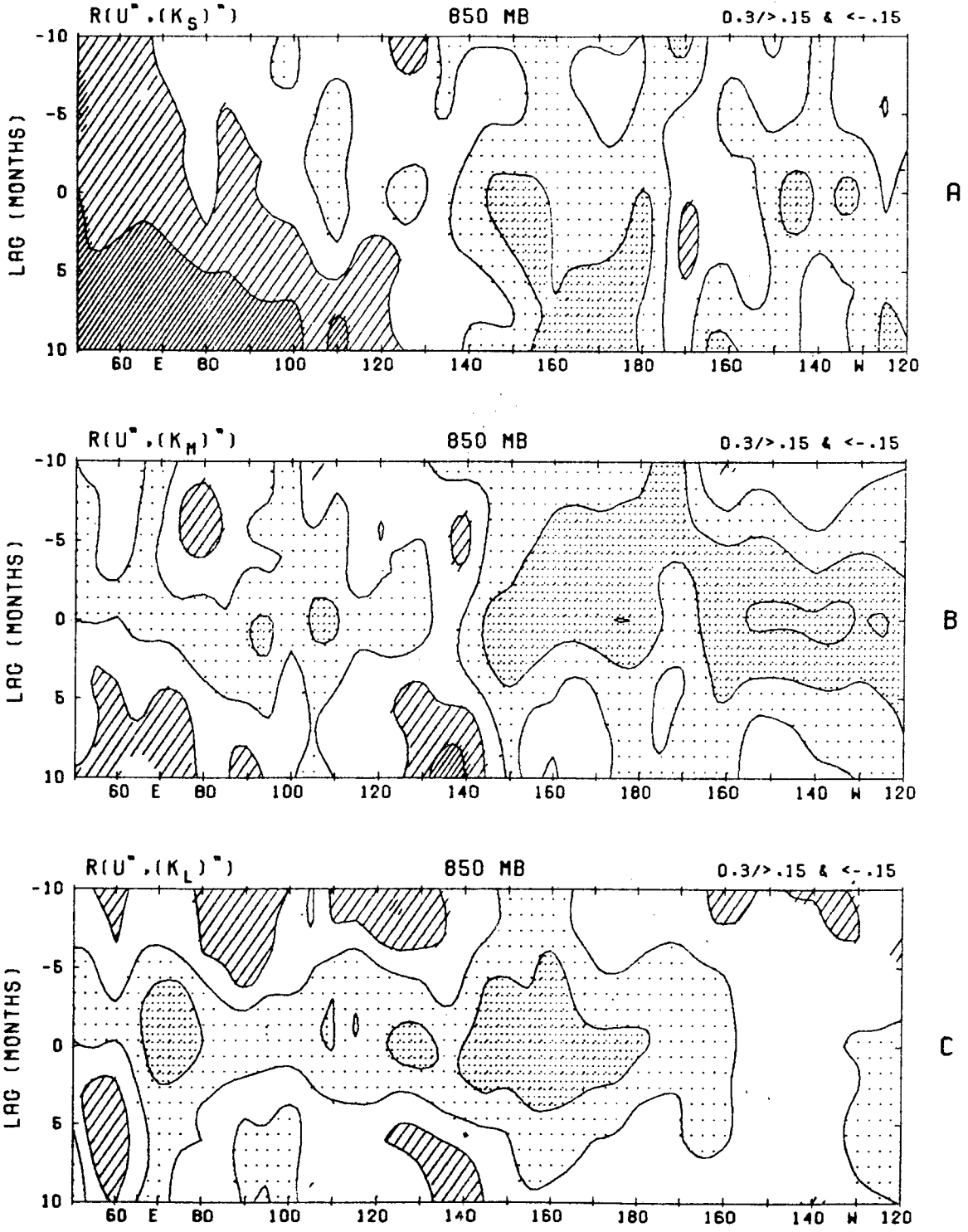

Fig. 5. (A) Lag correlation between u" and $K_S^{"}$ at the equator from 50°E to 120°W. The ordinate is for lag months, e.g., +10 mean $K_S^{"}$ lagging u" by 10 months. (B) For $K_M^{"}$. (C) For $K_L^{"}$. Interval is 0.3. Hatching (dark hatching) indicates regions of negative correlation less than -0.15 (-0.45). Mesh (dark mesh) is for positive correlation greater than +0.15 (+0.45).

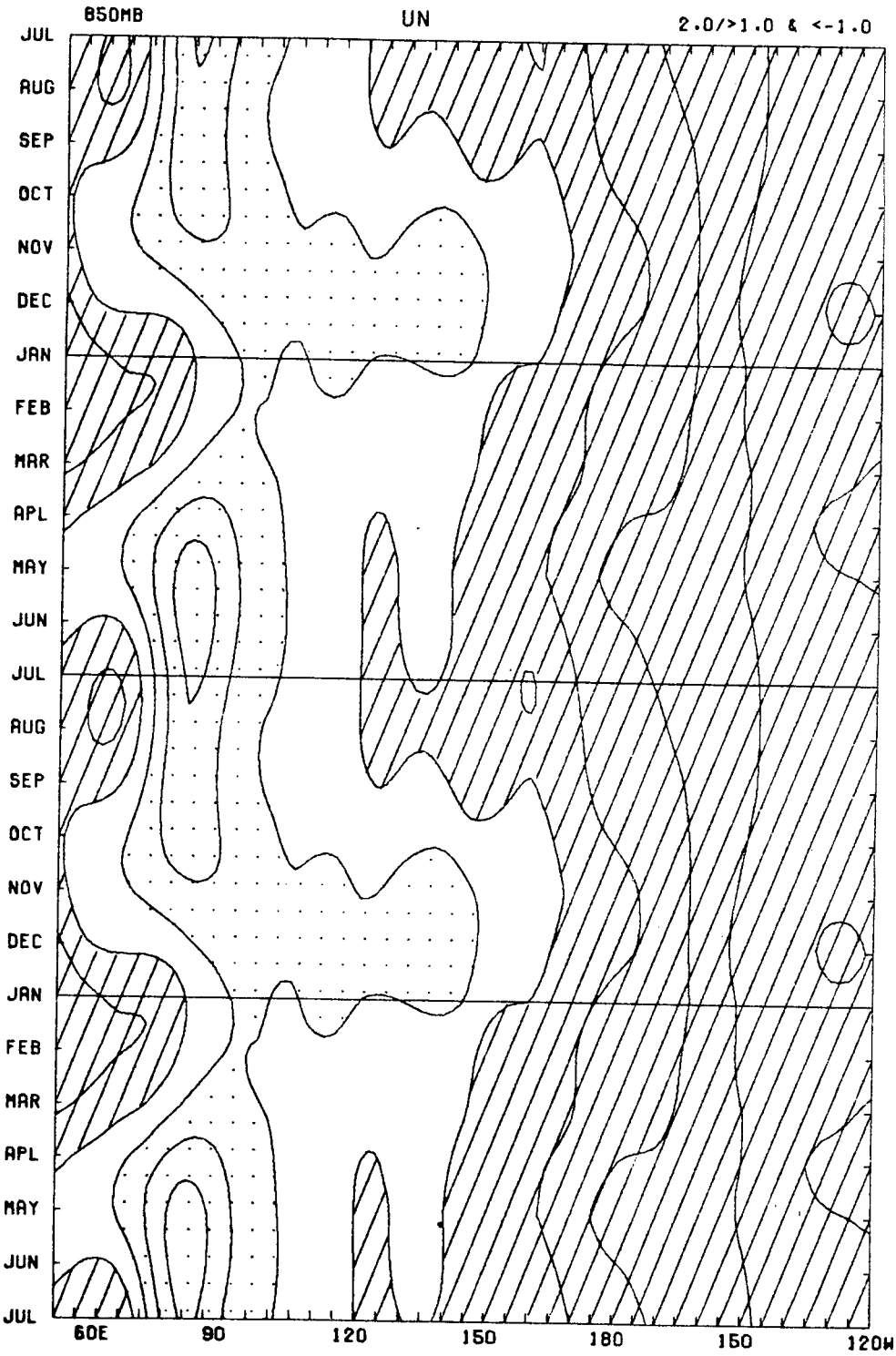

Fig. 6. Longitude-time section of u_n at the equator. Mesh (hatching) indicates values greater than +1 m s^{-1} (less than -1 m s^{-1}). Interval is 2 m s^{-1}.

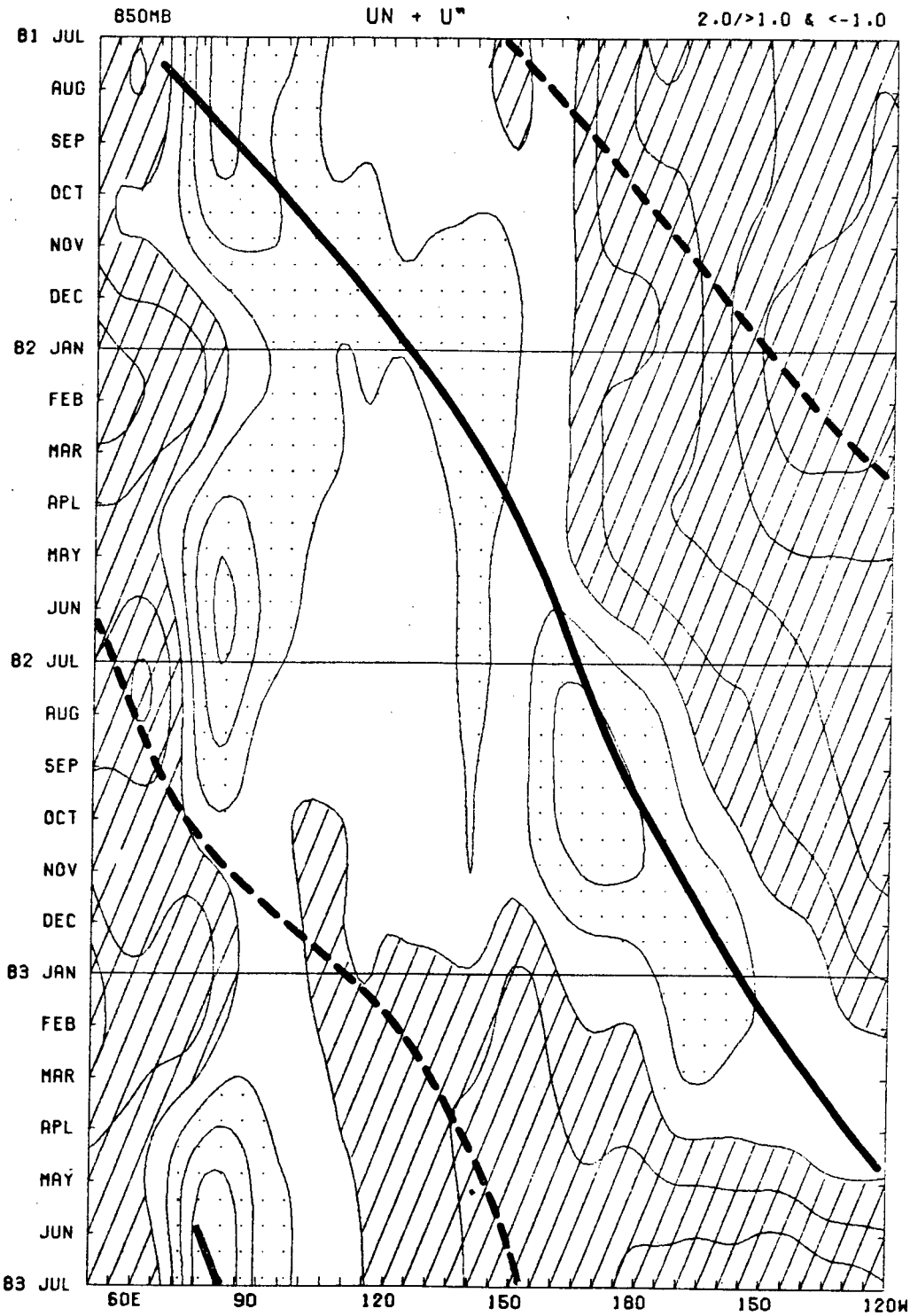

Fig. 7. As in Fig. 6, except for 3-month mean <u>, i.e., u_n + u". Heavy (dashed) lines indicate eastward propagation of westerly (easterly) u".

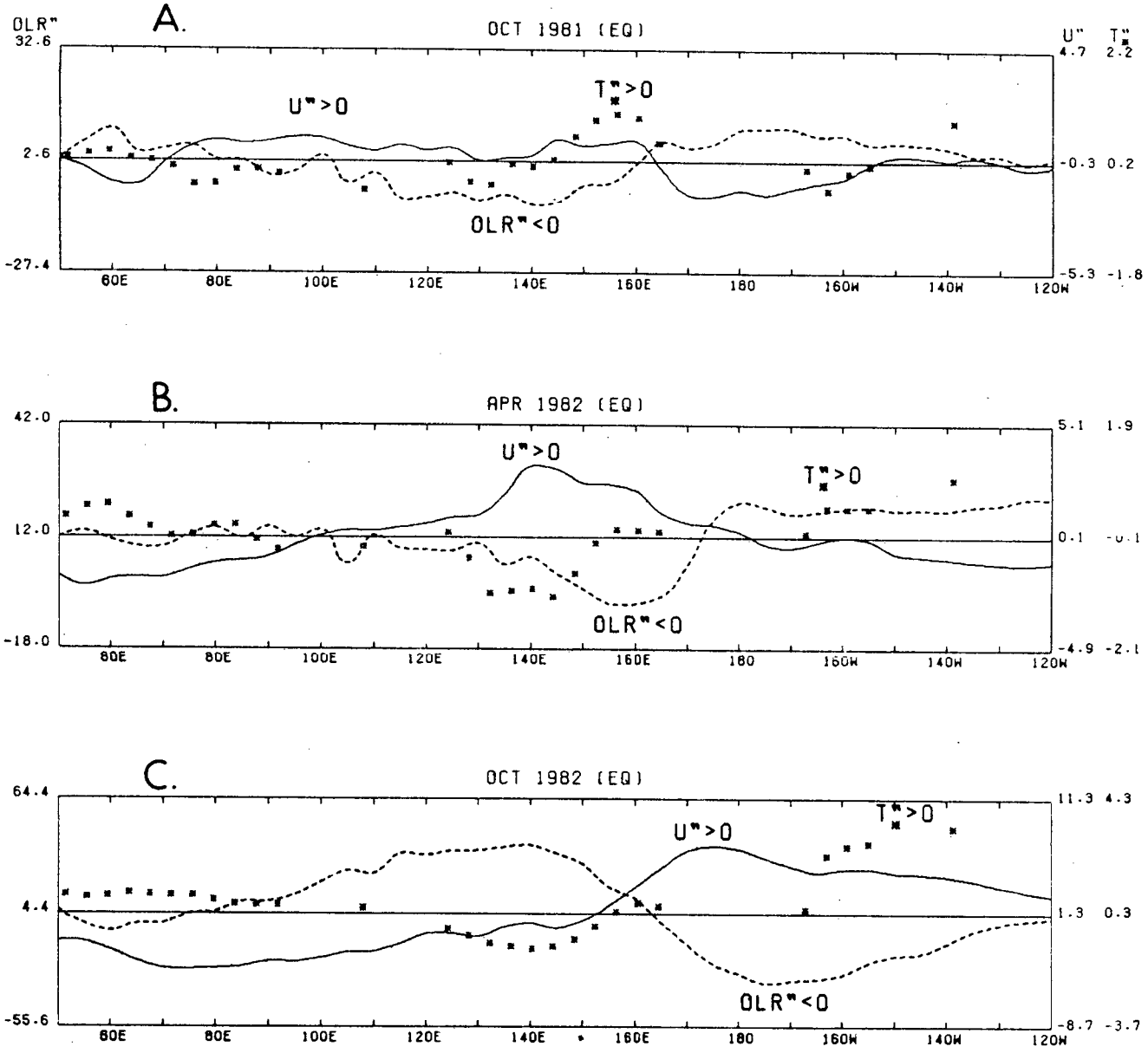

Fig. 8. Longitude profile of u" (m s^{-1}; full line), OLR" (W m^{-2}; dashed line), and $T^{"}_{*}$ (^{o}C; stars) along the equator from 50^{o}E-120^{o}W in October 1981 (A), April 1982 (B), and October 1982 (C).

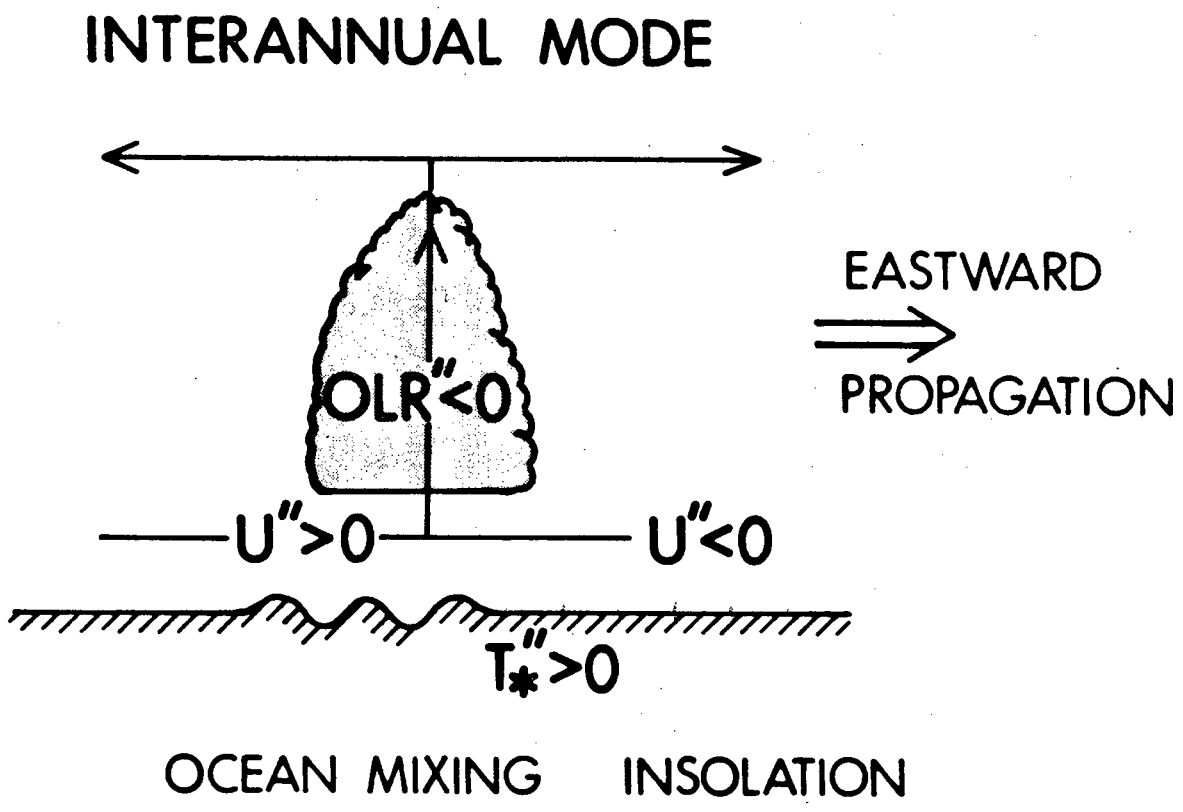

Fig. 9. Schematic diagram showing relationship between u", OLR", and T_*'' over an equatorial region of the Indian and Pacific Oceans.

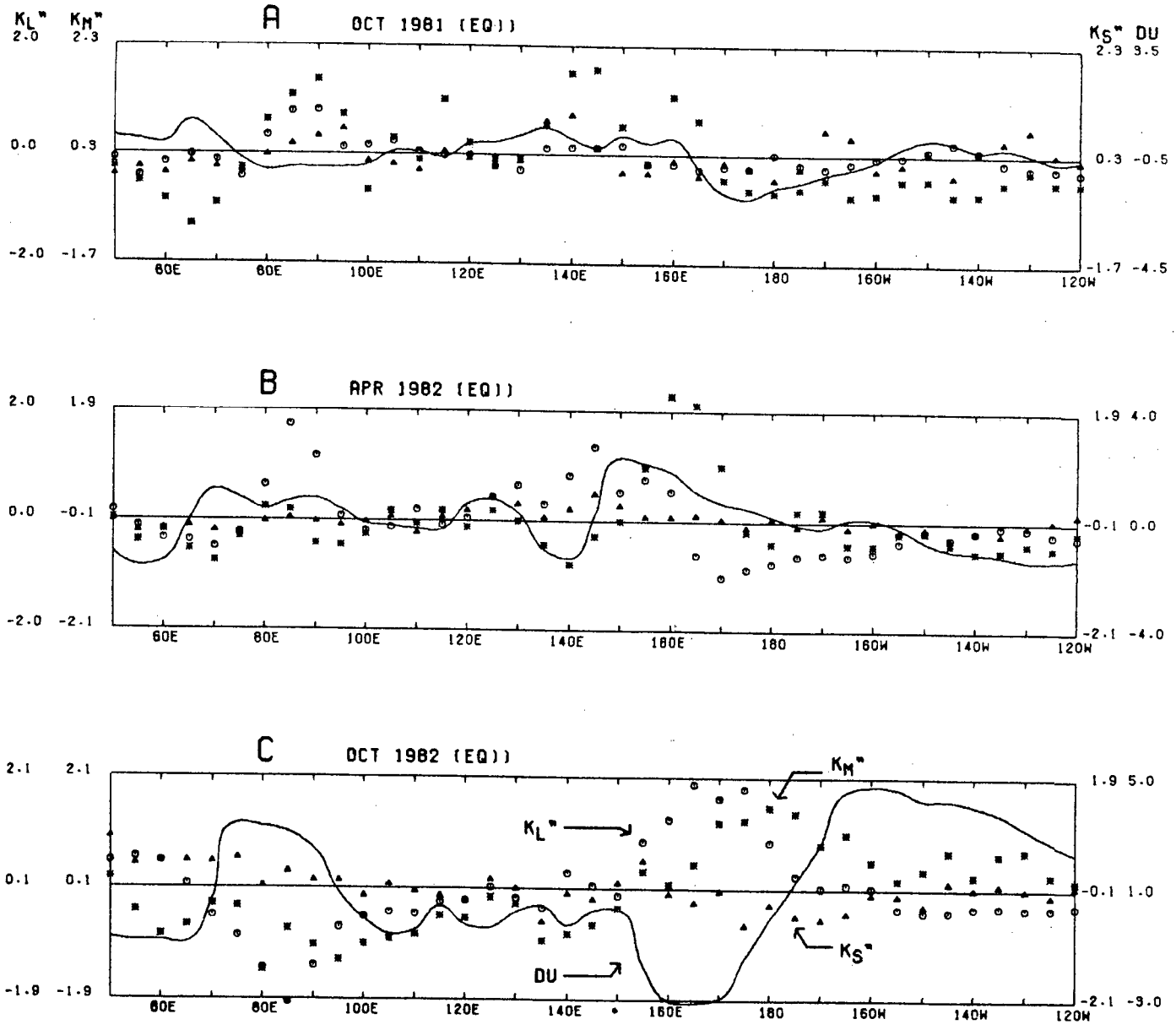

Fig. 10. As in Fig. 8, except for K''_L (m^2 s^{-2}; circles), K''_M (m^2 s^{-2}; stars), K''_S (m^2 s^{-2}; triangles), and DU (m s^{-1}; full line).